

# Orbitally driven east–west antiphasing of South American precipitation

Francisco W. Cruz<sup>1\*</sup>, Mathias Vuille<sup>2</sup>, Stephen J. Burns<sup>3</sup>, Xianfeng Wang<sup>4</sup>, Hai Cheng<sup>4</sup>, Martin Werner<sup>5</sup>, R. Lawrence Edwards<sup>4</sup>, Ivo Karmann<sup>1</sup>, Augusto S. Auler<sup>6</sup> and Hanh Nguyen<sup>2</sup>

**The variations of tropical precipitation are antiphased between the hemispheres on orbital timescales. This antiphasing arises through the alternating strength of incoming solar radiation in the two hemispheres, which affects monsoon intensity and hence the position of the meridional atmospheric circulation of the Hadley cells<sup>1–4</sup>. Here we compare an oxygen isotopic record recovered from a speleothem from northeast Brazil for the past 26,000 years with existing reconstructions of precipitation in tropical South America<sup>5–8</sup>. During the Holocene, we identify a similar, but zonally oriented, antiphasing of precipitation within the same hemisphere: northeast Brazil experiences humid conditions during low summer insolation and aridity when summer insolation is high, whereas the rest of southern tropical South America shows opposite characteristics. Simulations with a general circulation model that incorporates isotopic variations support this pattern as well as the link to insolation-driven monsoon activity. Our results suggest that convective heating over tropical South America and associated adjustments in large-scale subsidence over northeast Brazil lead to a remote forcing of the South American monsoons, which determine most of the precipitation changes in the region on orbital timescales.**

The Nordeste, a semi-arid region in northeastern Brazil, is known for its severe and recurrent droughts, which cause socioeconomic problems for millions of people. Observational and modelling studies have convincingly linked below-normal rainfall in the Nordeste during the rainy season (February, March and April) to periods of anomalously warm waters in the tropical North Atlantic sector, a weakened interhemispheric sea-surface-temperature gradient, an unusually far northward position of the intertropical convergence zone (ITCZ) and El Niño conditions in the tropical Pacific (for example refs 9,10).

Abrupt reduction of the Atlantic meridional overturning circulation and sea-ice expansion in the North Atlantic are viewed to be the cause of a southward displacement of the ITCZ (ref. 11), which promoted wet conditions in the Nordeste<sup>12</sup> and dry conditions in Venezuela<sup>13,14</sup> on millennial timescales. These episodic wet phases extended to the interior of the Nordeste, where they are recorded by short-lived speleothems/travertine growth phases<sup>15</sup>.

The long-term average climatic conditions in the Nordeste are primarily a result of the subtropical anticyclone in the South Atlantic and persistent subsidence related to the Nordeste Low in the upper troposphere. Monsoon systems tend to influence the equatorward portion of subtropical anticyclones to the east of

the monsoon rains through a Kelvin wave response<sup>16</sup>. A strong summer monsoon over South America strengthens the subtropical South Atlantic Anticyclone and leads to drier conditions in the Nordeste, whereas the opposite is the case during weak monsoons. The Nordeste Low, dynamically linked with large-scale subsidence over northeastern Brazil, is also formed and maintained as a direct linear response to condensational heating over the Amazon basin<sup>17,18</sup> and tropical Africa<sup>19</sup>. As the South American summer monsoon shows a strong sensitivity to summer insolation on orbital timescales<sup>2,6,20</sup>, precipitation in the Nordeste should in theory respond to insolation-driven monsoon variations as well.

Our results are based on a speleothem stable-isotope record from the northern part of the Nordeste that covers the past 26,000 years. Stalagmites were collected in Rainha, Furna Nova and Abissal caves, located at 05°36' S, 37°44' W, ~100 m a.s.l. and at ~100 km distance from the Atlantic coast in the Brazilian state of Rio Grande do Norte (Fig. 1). The isotopic composition of rainfall at this site is primarily influenced by the amount of rainfall and is characterized by a decrease in  $\delta^{18}\text{O}$  with increasing rainfall totals on interannual<sup>21</sup> and seasonal timescales, as clearly observed at the nearby GNIP-IAEA stations of Ceará Mirim ( $R^2_{\text{seasonal}} = 0.66$ ,  $p < 0.001$ ) and Fortaleza ( $R^2_{\text{seasonal}} = 0.79$ ,  $p < 0.001$ ).

The Rio Grande do Norte record (hereafter RN record) is a combination of five stalagmites, whose chronology is based on 48 radiometric ages, obtained with the application of U-series techniques on an inductively coupled plasma mass spectrometer (see Supplementary Table S1, Supplementary Fig. S5 and the Methods section for information). RN stable-isotope profiles represent an average of 25 years, with minimum and maximum resolution between 2 and 77 years. Values of  $\delta^{18}\text{O}$  vary greatly, from  $-8.39$  to  $-0.72\text{‰}$  ( $n = 1,274$ ) (Fig. 2). These stalagmites seem to have been deposited in isotopic equilibrium with the cave dripwater as indicated by the low correlation between  $\delta^{18}\text{O}$  and  $\delta^{13}\text{C}$  ( $R^2 = 0.14$  and  $R^2 = 0.08$  for RN1 and RN4, respectively,  $p = 0.001$ ). The good reproducibility between coeval stalagmite segments also supports this interpretation. The relatively large amplitude of  $\delta^{18}\text{O}$  rules out a major temperature effect or a significant influence of global ice volume on  $\delta^{18}\text{O}$  variations. Hence, we interpret the oxygen isotope ratios of RN mainly as a function of the isotopic composition of rainfall, with  $\delta^{18}\text{O}$  being inversely proportional to the relative changes in precipitation amount.

During the last glacial period, high  $\delta^{18}\text{O}$  values (mean of  $-2.91 \pm 0.57\text{‰}$  between 26 and 15.1 kyr BP) indicate predominantly dry conditions at our study site, consistent with results from Caço

<sup>1</sup>Instituto de Geociências, Universidade de São Paulo, Rua do Lago, 562, CEP 05508-080, São Paulo-SP, Brazil, <sup>2</sup>Department of Earth and Atmospheric Sciences, University at Albany, SUNY, 1400 Washington Ave, Albany, New York 12222, USA, <sup>3</sup>Department of Geosciences, Morrill Science Center, University of Massachusetts, Amherst, Massachusetts 01003, USA, <sup>4</sup>Department of Geology and Geophysics, University of Minnesota, Minneapolis, Minnesota 55455, USA, <sup>5</sup>Alfred Wegener Institute for Polar and Marine Research, Bussestr. 24, D-27570 Bremerhaven, Germany, <sup>6</sup>Instituto do Carste, Rua Kepler 385/04, Belo Horizonte, MG 30360-240, Brazil. \*e-mail: cbill@usp.br.

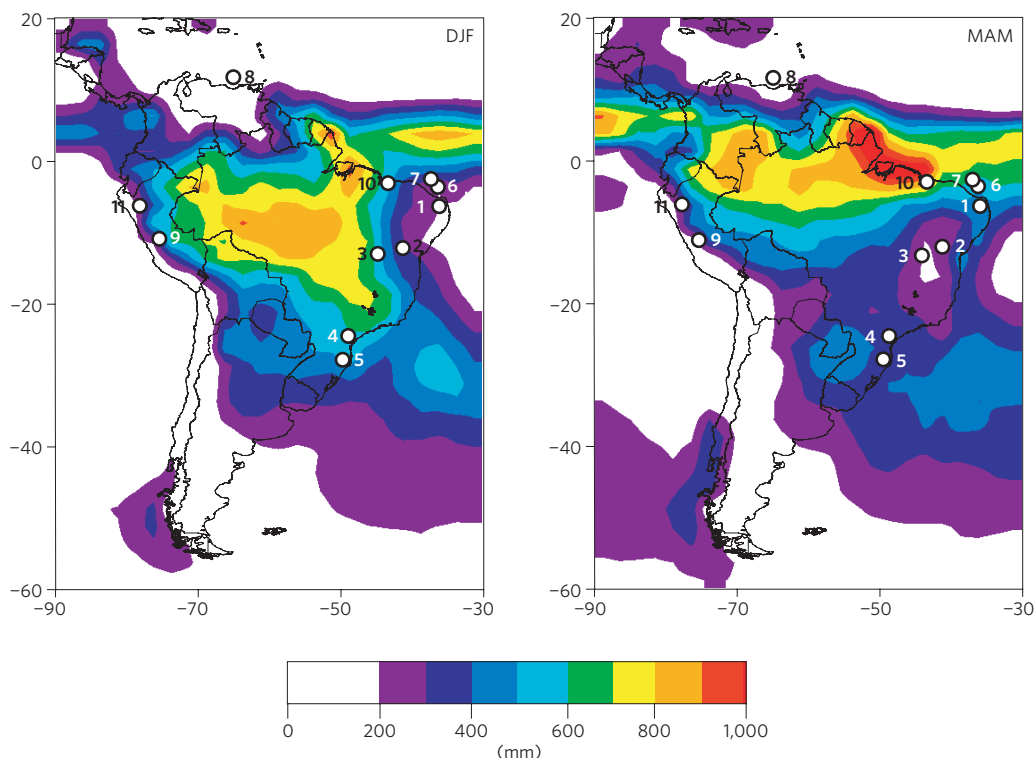


**Figure 1 | Long-term mean (1979–2000) Climate Prediction Center Merged Analysis of Precipitation seasonal precipitation totals (in mm) for December–February (left) and March–May (right).** Most of the precipitation over Brazil occurs in DJF and is related to the South American summer monsoon, whereas the eastern part of the Nordeste region is relatively dry. Precipitation in northeast Brazil is mainly associated with the southernmost position of the ITCZ in MAM. Numbers in the figure indicate locations mentioned in the text: 1—Rio Grande do Norte, 2—Toca da Boa Vista<sup>15</sup>, 3—Gruta do Padre<sup>24</sup>, 4—Santana cave<sup>20</sup>, 5—Botuverá cave<sup>4,6</sup>, 6 and 7—marine cores GeoB 3911-3 and Geo B 3104-1<sup>12</sup>, 8—Cariaco Basin, Venezuela<sup>13</sup>, 9—Lake Junin, Peru<sup>5</sup>, 10—Caço Lake<sup>22</sup>, 11—Cueva del Tigre Perdido<sup>8</sup>.

1 Lake<sup>22</sup> on the west side of the region (Fig. 1). This tendency is  
 2 interrupted by abrupt shifts to values as low as  $-5.5$  and  $-6.5$ ‰  
 3 from 25.9 to 25.0 kyr and from 17.3 and 15.1 kyr BP, respectively,  
 4 consistent with wet conditions during Heinrich events 2 (H2)  
 5 and 1 (H1), as suggested by marine and speleothem records and  
 6 commonly attributed to the shutdown of the Atlantic meridional  
 7 overturning circulation<sup>2,12,15,23</sup>. H1, in particular, is characterized  
 8 by high-amplitude  $\delta^{18}\text{O}$  variations of 6‰ that might be associated  
 9 with extreme changes from dry to wet conditions occurring  
 10 within the time span of a few years to decades between 17.3 and  
 11 16.4 kyr, followed by a prevalent wet climate between 16.4 kyr  
 12 and 15.1 kyr BP (Fig. 2).

13 No speleothem deposition was found in any cave between  
 14 15.1 and 13.2 kyr BP. This hiatus is probably associated with dry  
 15 conditions during the Bølling-Allerød interval, as also observed  
 16 in speleothem isotope records from the southwestern Nordeste<sup>24</sup>.  
 17 After the hiatus, the speleothems show a large variability in  $\delta^{18}\text{O}$  on  
 18 multidecadal to centennial timescales. Unlike speleothem records  
 19 from southern Brazil, however, no clear abrupt negative shift in  
 20  $\delta^{18}\text{O}$  is apparent in RN during the Young Dryas (YD) chronozone.  
 21 Oceanic conditions during the YD event probably had less of an  
 22 impact on palaeoprecipitation in the Nordeste than during H1,  
 23 which is supported by a lesser anomaly in Fe/Ca ratios of core GeoB  
 24 3912-1 during the YD than during H1 (ref. 12) and cave calcite  
 25 growth phases during H1, although only travertine deposition  
 26 occurred during the YD elsewhere in the Nordeste<sup>15</sup>.

27 In general, the  $\delta^{18}\text{O}$  variations after 13.2 kyr bear a striking  
 28 resemblance to summer insolation at 10° S, with the lowest  $\delta^{18}\text{O}$   
 29 values between 10.5 and 5.0 kyr BP, when insolation was at its min-  
 30 imum (Fig. 2). The transition from the middle to the late Holocene  
 31 is marked by an abrupt increase in the  $\delta^{18}\text{O}$  of  $\sim 1.5$ ‰ at about

5 kyr BP that persists until 4.2 kyr BP, when most of the collected  
 stalagmites stopped growing. Only the FN1 stalagmite covers the  
 past 3.7 kyr BP, and it shows a gradual increase in  $\delta^{18}\text{O}$  values to the  
 present, indicating dry late Holocene conditions in the Nordeste,  
 similar to what is observed in Cariaco Basin, Venezuela (Fig. 2)<sup>14</sup>.

Our record indicates a predominantly wet climate in the  
 semi-arid Nordeste during the early and mid-Holocene, a result that  
 was not documented in the earlier discontinuous speleothem  
 record from a more southern location in the Nordeste<sup>15</sup>. Our  
 results are also in contrast to previous suggestions of dry conditions  
 throughout the Holocene, on the basis of the interpretation of very  
 low Ti/Ca ratios in nearby marine cores<sup>12</sup>. Finally, our results are  
 opposite to climate changes documented in the central Andes<sup>5</sup>,  
 western Amazon<sup>8</sup> and southeastern Brazil<sup>2,6,20</sup>, and suggest an  
 antiphased relationship between precipitation in northeast Brazil  
 and the rest of tropical South America during the Holocene.

Our speleothem results are supported by experiments using  
 an isotope-enabled General Circulation Model<sup>25</sup>, which indicates  
 significantly wetter conditions at 6 kyr BP over the Nordeste,  
 compared with today (Fig. 3a), whereas conditions are drier over  
 the rest of tropical South America, consistent with proxy records  
 from southern Brazil<sup>2,6,7</sup>, the western Amazon<sup>8</sup> and the tropical  
 Andes<sup>5</sup>. The model also produces more negative  $\delta^{18}\text{O}$  values over  
 the Nordeste, probably a result of the intensified precipitation  
 (Fig. 3b). The spatial pattern of more negative  $\delta^{18}\text{O}$  over the  
 Nordeste, but more enriched values over the tropical Andes during  
 the early to mid-Holocene, is consistent with stable isotopic records  
 from lakes and ice cores in the Andes<sup>5,26</sup> and is a pattern that can also  
 be observed today during weak monsoon seasons<sup>27</sup>.

Precipitation in the Nordeste occurs almost exclusively between  
 December and May, which is correctly simulated by the model (see

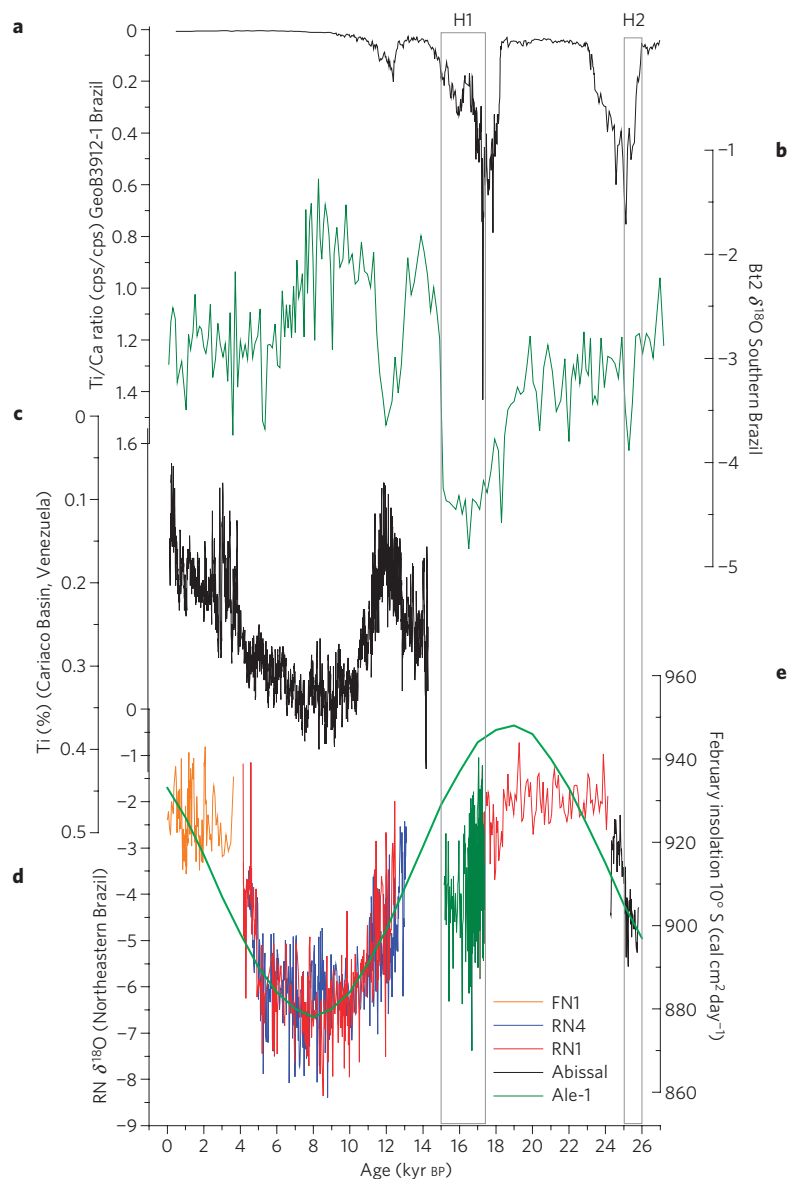


**Figure 2 | a–e**, Comparison between Ti/Ca ratios from Marine Core 3912-1 (ref. 17) (a), Bt2 speleothem  $\delta^{18}\text{O}$  record from Botuverá cave, Southern Brazil<sup>6</sup> (b), Ti record from Cariaco Basin<sup>14</sup> (c), RN record (d) and February insolation at 10° S (e).

1 Supplementary Fig. S1), although precipitation is overestimated in  
 2 January and February. There is no evidence from proxy data that  
 3 seasonality in precipitation was different during the mid-Holocene,  
 4 nor does it change in our model (see Supplementary Fig. S2a).  
 5 We therefore interpret the observed change in precipitation and  
 6  $\delta^{18}\text{O}$  in the Nordeste to be related to wetter conditions and a  
 7 more negative isotopic composition of rainfall during the peak of  
 8 the monsoon phase, when  $\delta^{18}\text{O}$  values were 1–2‰ more negative  
 9 (see Supplementary Fig. S2b). The wet conditions over northeast  
 10 Brazil during the mid-Holocene are also supported by coupled  
 11 atmosphere–ocean global climate model simulations<sup>28–30</sup> and  
 12 experiments performed within the framework of the Paleoclimate  
 13 Modeling Intercomparison Project (<<http://pmip2.lsce.ipsl.fr/>>).

14 Increased aridity at this southern hemisphere site (5° S) occurred  
 15 at times when the South American monsoon was enhanced over  
 16 southern Brazil<sup>2,6</sup>, the western Amazon<sup>8</sup> and the tropical Andes<sup>5</sup>,  
 17 and when the ITCZ was displaced southward, causing a deficit  
 18 in precipitation during the late Holocene in northern South  
 19 America<sup>14</sup>. Therefore, the meridional movement of the ITCZ  
 20 alone cannot account for our observed long-term variations in

precipitation over the Nordeste during the Holocene; otherwise we  
 would expect to see an inter-hemispheric antiphased relationship  
 with the northern tropical sites. Instead, the antiphased relationship  
 between summer insolation and speleothem  $\delta^{18}\text{O}$  (Fig. 2) suggests  
 that precipitation over northeast Brazil is also modulated by  
 monsoon intensity on orbital timescales, albeit antiphased with  
 the core monsoon regions. Intense convective activity and vertical  
 updraft in the core region of the monsoon during its mature  
 phase (austral summer) requires compensating subsidence in  
 surrounding regions (see Supplementary Fig. S3). Latent heat  
 release during monsoon precipitation (condensational heating)  
 affects the strength of the equatorward portion of the subtropical  
 anticyclone to the east over northeast Brazil<sup>16</sup> and is dynamically  
 tied to the upper-tropospheric Nordeste low, responsible for  
 large-scale subsidence and aridity over the region<sup>17</sup>. During a  
 weaker monsoon, on the other hand, subsidence and aridity  
 over northeast Brazil will be reduced (see Supplementary Fig.  
 S3). Indeed, our model simulations are entirely consistent with  
 this theory. The Nordeste Low is much less pronounced in our  
 mid-Holocene experiment than in the control run (Fig. 3c) and

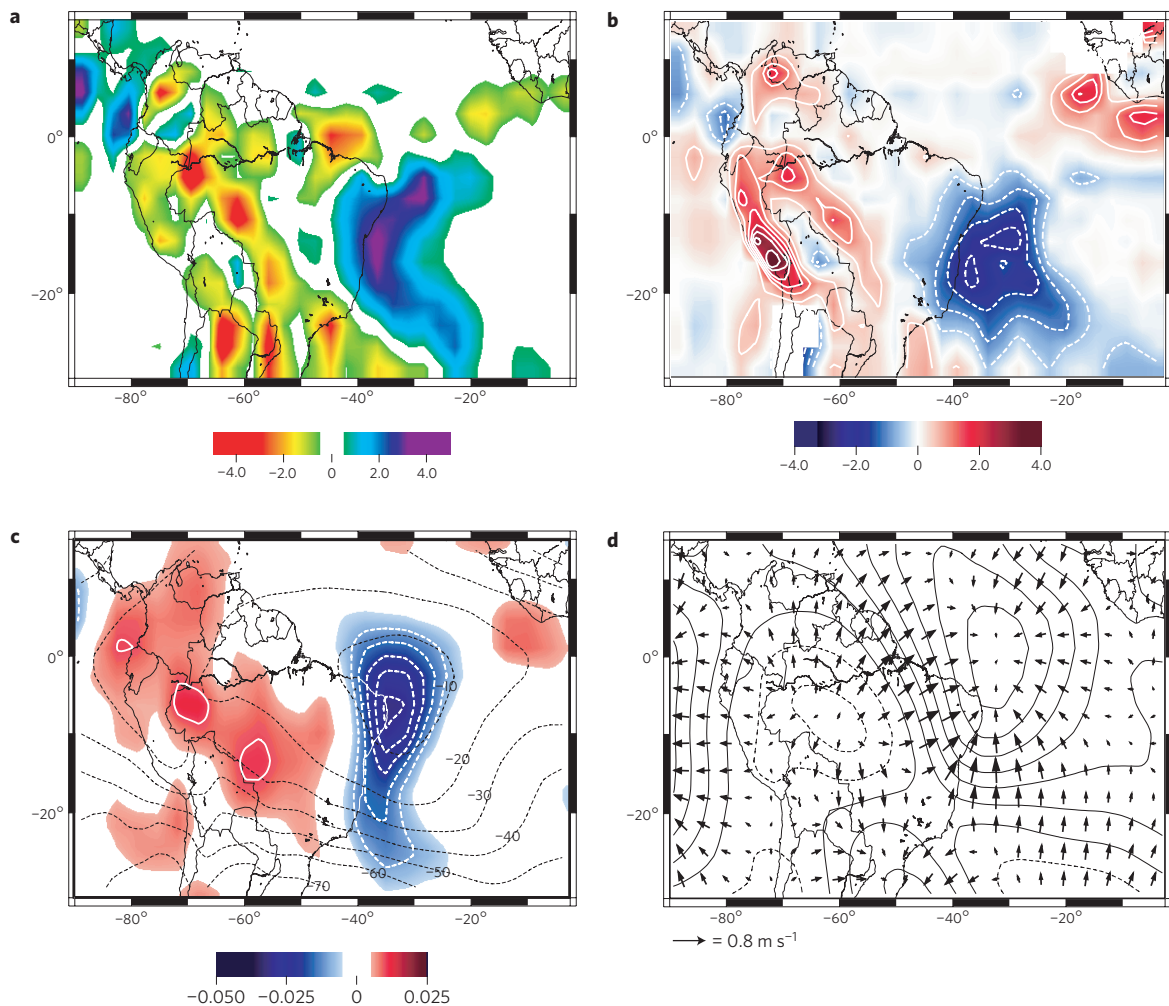


**Figure 3** | **a**, Difference in austral summer and autumn (DJFMAM) precipitation ( $\text{mm day}^{-1}$ ) between 6 kyr BP and the present as simulated with ECHAM-4. The control run is based on a 10-year integration forced with modern sea-surface temperatures and greenhouse gases; the mid-Holocene simulation is a 10-year integration on the basis of orbital configuration at 6 kyr BP and preindustrial greenhouse-gas levels, but with modern vegetation and sea-surface temperature. **b**, As in **a** but for  $\delta^{18}\text{O}$  (in ‰). The contour interval is  $0.5\text{‰}$ , the zero contour is omitted and negative contours are dashed. **c**, As in **a**, but for 250 hPa geopotential height (black contours; the contour interval is 10 m and negative contours dashed) and 500 hPa vertical velocity (white contours and colour shading; the contour interval is  $1.25 \times 10^{-2} \text{ Pa s}^{-1}$ ). **d**, As in **a**, but for 850 hPa velocity potential (the contour interval is  $2.0 \times 10^5 \text{ m}^2 \text{ s}^{-1}$ ; negative contours are dashed) and divergent wind component ( $\text{m s}^{-1}$ , scale in lower left).

1 subsidence is greatly reduced over northeast Brazil in response to  
 2 reduced summer insolation and monsoon precipitation (Fig. 3c).  
 3 The low-level divergent circulation over tropical South America  
 4 is characterized by anomalous large-scale divergence over the  
 5 Amazon basin and anomalous convergence over northeast Brazil  
 6 and the adjacent equatorial Atlantic at 6 kyr BP (Fig. 3d). A near-  
 7 equatorial cross-section of vertical velocity and divergence from  
 8 South America to Africa confirms that changes in insolation forcing  
 9 at 6 kyr BP produce a reduction in low-level convergence and  
 10 vertical ascent over both continents, which are balanced by reduced  
 11 subsidence over coastal and oceanic areas (see Supplementary Fig.  
 12 S4). These theoretical and model-based interpretations provide a  
 13 dynamically consistent explanation for a continental forcing of  
 14 past rainfall variability in northeast Brazil, as indicated by our  
 15 speleothem- $\delta^{18}\text{O}$  record.

16 The lack of a clear match between the  $\delta^{18}\text{O}$  of RN and  
 17 insolation during the Last Glacial Maximum suggest that changes  
 18 in Atlantic meridional overturning circulation and sea ice and  
 19 temperatures in the high northern latitudes are the dominant  
 20 control on ITCZ location, wet season rainfall and circulation  
 21 at that time (Fig. 2), as previously suggested on the basis of

Mg/Ca and Sr/Ca variations in the Bt2-speleothem record<sup>7</sup>. Absent  
 glacial or deglacial conditions however, precipitation in northeast  
 Brazil was antiphased with the rest of tropical South America  
 throughout the Holocene owing to insolation-driven changes in  
 monsoon circulation. These results demonstrate that orbitally  
 driven antiphased relationships in precipitation are not limited to  
 interhemispheric antiphasing as demonstrated previously, but may  
 well occur within the same hemisphere.

## Methods

Age determinations were carried out at the Minnesota Isotope Laboratory  
 (USA), using a sector field inductively coupled plasma mass spectrometer  
 (Thermo-Finnigan ELEMENT), according to the procedures described in  
 Supplementary Information, S1. Forty-eight samples weighing between 100 and  
 500 mg were dissolved and equilibrated with a  $^{236}\text{U}$ - $^{233}\text{U}$ - $^{229}\text{Th}$  spike and then  
 separated and purified using methods described in Supplementary Information,  
 S2. Initial  $^{230}\text{Th}$  values were corrected with a typical bulk earth ratio, that is, atomic  
 ratio of  $^{230}\text{Th}/^{232}\text{Th} = 4.4 \pm 2.2 \text{ p.p.m.}$ . U-Th isotopic data and ages are shown  
 in Supplementary Table S1. Some subsamples show age errors between 1 and  
 5%, because of high detrital Th and low U concentrations in the samples (see  
 Supplementary Fig. S5). All ages are reported with  $2\sigma$  errors (95% confidence  
 limits). Subsamples of FN1 stalagmite presenting high and low  $^{238}\text{U}$  concentrations  
 correspond to aragonitic and calcitic layers, respectively.

Oxygen isotope ratios are expressed in  $\delta$  notation, the permil deviation from the VPDB standard. For example, for oxygen,  $\delta^{18}\text{O} = [((^{18}\text{O}/^{16}\text{O})_{\text{sample}} / (^{18}\text{O}/^{16}\text{O})_{\text{VPDB}}) - 1] \times 1,000$ . For each measurement, approximately 200  $\mu\text{g}$  of powder was drilled from the sample and analysed with an on-line, automated, carbonate preparation system linked to a Finnigan Delta XL ratio mass spectrometer at the University of Massachusetts (speleothem samples FN1, RN1 and RN4) and to a Finnigan Delta Plus Advantage at the University of São Paulo (speleothem samples ALE1 and Abissal). Reproducibility of standard materials is 0.08‰ for  $\delta^{18}\text{O}$ .

Received 11 September 2008; accepted 27 January 2009; published online XX Month XXXX

## References

- Thompson, L. G. *et al.* Tropical ice core records: Evidence for asynchronous glaciation on Milankovitch timescales. *J. Quat. Sci.* **20**, 723–733 (2005).
- Wang, X. *et al.* Millennial-scale precipitation changes in southern Brazil over the past 90,000 years. *Geophys. Res. Lett.* **241**, 699–706 (2007).
- Kutzbach, J. E., Liu, X., Liu, Z. & Chen, G. Simulation of the evolutionary response of global summer monsoons to orbital forcing over the past 280,000 years. *Clim. Dyn.* **30**, 567–579 (2008).
- Wang, X. *et al.* Interhemispheric anti-phasing of rainfall during the last glacial period. *Quat. Sci. Rev.* **25**, 3391–3403 (2006).
- Seltzer, G., Rodbell, D. & Burns, S. J. Isotopic evidence for Late Glacial and Holocene hydrologic change in tropical South America. *Geology* **28**, 35–38 (2000).
- Cruz, F. W. *et al.* Insolation-driven changes in atmospheric circulation over the past 116,000 years in subtropical Brazil. *Nature* **434**, 63–66 (2005).
- Cruz, F. W. *et al.* Evidence of rainfall variations in southern Brazil from trace element ratios (Mg/Ca and Sr/Ca) in a Late Pleistocene stalagmite. *Geochim. Cosmochim. Acta* **71**, 2250–2263 (2007).
- van Breukelen, M. R., Vonhof, H. B., Hellstrom, J. C., Wester, W. C. G. & Kroon, D. Fossil dripwater in stalagmites reveals Holocene temperature and rainfall variation in Amazonia. *Earth Planet. Sci. Lett.* **275**, 54–60 (2008).
- Nobre, P. & Shukla, J. Variations of sea surface temperature, wind stress, and rainfall over the tropical Atlantic and South America. *J. Clim.* **9**, 2464–2479 (1996).
- Hastenrath, S. Interannual and longer-term variability of upper-air circulation in the Northeast Brazil—Tropical Atlantic Sector. *J. Geophys. Res.* **105**, 7327–7335 (2000).
- Claussen, M., Ganopolski, A., Brovkin, V., Gerstengarbe, F.-W. & Werner, P. Simulated global-scale response of the climate system to Dansgaard/Oeschger and Heinrich events. *Clim. Dyn.* **21**, 361–370 (2003).
- Arz, H. W., Pätzold, J. & Wefer, G. Correlated millennial-scale changes in surface hydrography and terrigenous sediment yield inferred from last glacial marine deposits off northeastern Brazil. *Quat. Res.* **50**, 157–166 (1998).
- Peterson, L. C., Haug, G. H., Hughen, K. A. & Röhl, U. Rapid changes in the hydrologic cycle of the tropical Atlantic during the last glacial. *Science* **290**, 1947–1951 (2000).
- Haug, G. H., Hughen, K. A., Sigman, D. M., Peterson, L. C. & Röhl, U. Southward migration of the intertropical convergence zone through the Holocene. *Science* **293**, 1304–1308 (2001).

- Wang, X. *et al.* Wet periods in northeastern Brazil over the past 210 kyr linked to distant climate anomalies. *Nature* **432**, 740–743 (2004).
- Rodwell, M. J. & Hoskins, B. J. Subtropical anticyclones and summer monsoons. *J. Clim.* **14**, 3192–3211 (2001).
- Lenters, J. D. & Cook, K. H. On the origin of the Bolivian High and related circulation features of the South American climate. *J. Atmos. Sci.* **54**, 656–677 (1997).
- Chen, T. C., Weng, S. P. & Schubert, S. Maintenance of austral summertime upper-tropospheric circulation over tropical South America: The Bolivian High-Nordeste Low system. *J. Atmos. Sci.* **56**, 2081–2100 (1999).
- Hagos, S. M. & Cook, K. H. Influence of surface processes over Africa on the Atlantic marine ITCZ and South American precipitation. *J. Clim.* **18**, 4993–5010 (2005).
- Cruz, F. W., Burns, S. J., Karmann, I., Sharp, W. D. & Vuille, M. Reconstruction of regional atmosphere circulation features during the late Pleistocene in subtropical Brazil from oxygen isotope composition of speleothems. *Earth Planet. Sci. Lett.* **248**, 494–506 (2006).
- Vuille, M., Bradley, R. S., Werner, M., Healy, R. & Keimig, F. Modeling  $\delta^{18}\text{O}$  in precipitation over the tropical Americas: 1. Interannual variability and climatic controls. *J. Geophys. Res.* **108**, 4174 (2003).
- Sifeddine, A. *et al.* A 21000 cal years paleoclimatic record from Caço Lake, Northern, Brazil: Evidence from sedimentary and pollen analyses. *Palaeogeogr. Palaeoclimatol. Palaeoecol.* **189**, 25–34 (2003).
- Jaeschke, A., Rühlemann, C., Arz, H., Heil, G. & Lohmann, G. Coupling of millennial-scale changes in sea surface temperature and precipitation off northeastern Brazil with high-latitude climate shifts during the last glacial period. *Paleoceanography* **22**, PA4206 (2007).
- Wang, X., Edwards, R. L., Auler, A. S., Cheng, H. & Ito, E. Millennial-scale interhemispheric asymmetry of low-latitude precipitation: Speleothem evidence and possible high-latitude forcing. *Geophys. Monogr. Ser.* **173**, 279–293 (2007b).
- Hoffmann, G., Werner, M. & Heimann, M. Water isotope module of the ECHAM atmospheric general circulation model: A study on timescales from days to several years. *J. Geophys. Res.* **103**, 16871–16896 (1998).
- Thompson, L. G. *et al.* Late Glacial stage and Holocene tropical ice core records from Huascarán, Peru. *Science* **269**, 46–50 (1995).
- Vuille, M. & Werner, M. Stable isotopes in precipitation recording South American summer monsoon and ENSO variability—observations and model results. *Clim. Dyn.* **25**, 401–413 (2005).
- Harrison, S. P. *et al.* Mid-Holocene climates of the Americas: A dynamical response to changed seasonality. *Clim. Dyn.* **20**, 663–688 (2003).
- Liu, Z., Otto-Bliesner, B., Kutzbach, J., Li, L. & Shields, C. Coupled climate simulation of the evolution of global monsoons in the Holocene. *J. Clim.* **16**, 2472–2490 (2003).
- Liu, Z., Harrison, S. P. & Kutzbach, J. E. Otto-Bliesner, Global monsoons in the mid-Holocene and oceanic feedback. *Clim. Dyn.* **22**, 157–182 (2004).

## Additional information

Supplementary Information accompanies this paper on [www.nature.com/naturegeoscience](http://www.nature.com/naturegeoscience). Reprints and permissions information is available online at <http://npg.nature.com/reprintsandpermissions>. Correspondence and requests for materials should be addressed to F.W.C.